NUMERICAL ANALYSIS ON SHELL-SIDE PERFORMANCES OF A SHELL AND TUBE HEAT EXCHANGER WITH STAGGERED BAFFLES

Sushant Prajapati
Asst. Professor ,Department of Mechanical Engineering
K.J. Institute of Engineering and Technology, Savli

Abstract: This work is proposed to possessing the characteristics of the simple fabrication of the shell and tube heat exchangerwith segmental baffles (STHX-SG) and thehelical flow of the shell and tube heat exchanger with continuous helical baffles (STHX-CH) and a shell and tube heat exchanger with staggered baffles (STHX-ST).The baffles of the STHX-ST are arranged according to a certain rule that the adjacentbaffles are staggered by a constant counter clockwise or clockwise angle in sequence. Comparisons of the heat transfer performance and pressure drop among the STHX-SG, STHX-CH, and STHX-ST are firstly carried out. Results show that the comprehensive performance of the STHX-ST is superior the STHX-SGand STHX-CH. The parametric studies about the baffle cut d and staggered angle b are conducted forthe STHX-ST.
Keywords: Heat transfer enhancement, Shell and tube heat exchanger, Numerical simulation

I. INTRODUCTION

To achieve the purpose of the energy saving and emission reduction, heat exchangers play a essencial role in various modern industry, such as chemical processing, and waste heat recovery. The shell and tube type heat exchanger (STHX) is one of the most widely used heat exchangers owing to its versatile usability, easy maintenance, high-pressure resistance, and high-temperature resistance [1]. The flow manner of the working fluid in the shell-can be divided into three types:, the longitudinal flow, the cross flow and the helical flow. The conventional shell and tube heat exchanger with segmental baffles (STHX-SG), of which a cross flow is presented in the shell-side as illustrated in Fig. 1(a), is the most common STHX because of its simple installation, low cost, and high heat transfer performance. However, there are some disadvantages, such as the high flow resistance, the flow induced vibration, and dead zones for the STHX-SG [2]. A variety of studies have been conducted to improve the comprehensive performance of heat exchangers by enhancing the heat transfer performance or reducing the flow resistance by researchers from all over the world [7–11]. Particularly, the shell and tube heat exchanger with helical baffles was invented by Lutcha et al. [12] and commercialized by ABB Lummus Global Inc [13]. Afterwards, more and more improved structures and measures were developed with respect to the helical flow manner [14–17]. Typically, Wang et al. [18–21] proposed a shell and tube heat exchanger with continuous helical baffles (STHX-CH), and the ideal helical flow was generated in the shell-side, as depicted in Fig. 1(b). However, the complexity of the fabrication about helical baffles was unavoidable, which increased the manufacturing cost relative tothe STHX-SG, obviously. Mellal et al. [22] investigated the effect of the baffles orientation preliminarily for the STHX, and the results showed that the case of baffle orientation angle of 180_ and baffle spacing of 64 mm, i.e., the conventional STHX-SG, is the optimal structure. determined the best configurations for the tube inserted with porous media using Genetic Algorithm (GA). Cavazzuti and Corticelli [24] proposed a robust automated method for the design of two-dimensional enhanced surfaces. Abdollahi and Shams however, an integrated research for the combination of the STHX-SG and helical flow is not discussed. Basing on the above studies, we propose a shell and tube heat exchanger with staggered baffles (STHX-ST) in view of taking the advantage of both the simple fabrication of the STHX-SG and the helical flow of STHX-CH, as outlined in Fig. 1(c).

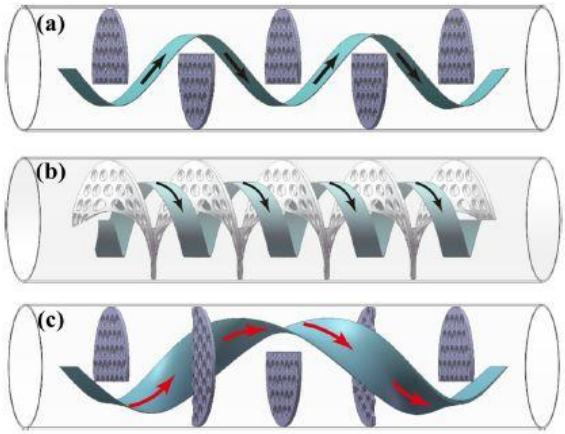

Fig :1: schmatic diagram of 1)STHX-SG 2)STHX-CH 3) STHX-ST

In the STHX-ST, the baffles are arrayed according to a certain rule that the adjacent baffles are staggered by a constant clockwise or counter clockwise angle in sequence. The fabrication and installation for staggered baffles are quite simple compared with those for helical baffles. Obviously, the baffle cut d, staggered angle b between the adjacent baffles, and number of baffles n, as illustrated in Fig. 2, have a significant effect on the comprehensive performance of the STHX-ST. The baffle cut is defined as the ratio of the cut height of the circular baffle and the inner diameter of the shell. The parametric studies about the effects of the d and b are also carried out This paper is organized as follows: (1) In Section 2, the numerical method,

adopted to verify the advantages of the STHX-ST, is outlined. (2) In Section 3, the analysis and comparison of the simulation results are performed for the STHX-SG, STHX-CH, and STHX-ST; and then, effects of the baffle cut d and staggered angle b are discussed for the STHX-ST; (3) Conclusions are briefly summarized in Section 4.

II. MODEL DESCRIPTION

Assumptions (1) The thickness of baffles is ignored; (2) The leakage flows, between baffles and the inner wall of the shell, and between baffles and the outer wall of tubes, are neglected; (3) The flow in the shell-side is in the turbulent region; (4) The outer walls of three heat exchangers are well-insulated, i.e., the heat flux to the surrounding is equal to zero.

2.1. Physical models

The whole model of the shell-side is adopted as the computational domain according to Ref. [26], in which Yang et al. indicated that the whole model had a high accuracy to predict the heat transfer performance and pressure drop. Physical models and parameters of the STHX-SG, STHX-CH, and STHX-ST, are depicted in Fig. 3.

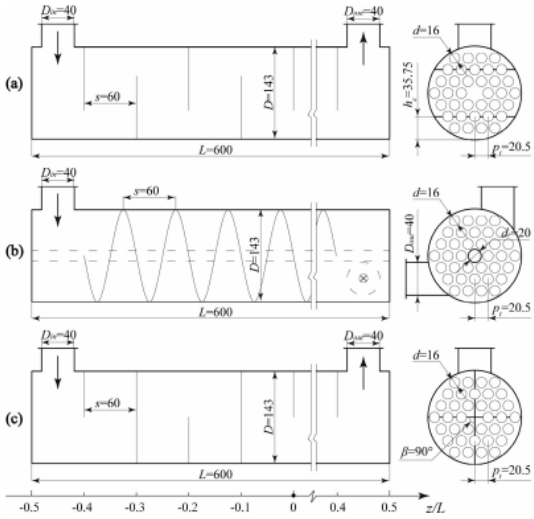

Fig 3: Geometry parameters of three STHX models (a) STHX-SG(b)STHX-CH(c)STHX-ST

The same diameter of the shell, diameter and position of inlet/outlet nozzles, and effective length of tubes are designed for three STHX models. The triangular tube layout with thirty-six identical tubes is applied for each STHX. The centre rod is set in the STHX-CH considering the actual installation of continuous helical baffles. Furthermore, nine baffles are set in the STHX-SG and STHX-ST, and the baffle spacing is equal to the helical pitch of the helical baffle in the STHX-CH model. As depicted in Fig. 3(c), semicircular baffles and vertical arrangement between adjacent baffles, i.e., the baffle cut d = 0.5, staggered angle b = 90_, and number of baffles n = 9 is designated as the original research object for the STHX-ST. To simplify the geometric structure and numerical computation,

2.2. Numerical simulation

2.2.1. Governing equations

The flow and heat transfer in the shell-side are assumed steady, and the gravity of the working fluid is ignored. In accordance with forementioned assumptions, governing equations in relation to the mass, momentum, and energy for numerical computations can be simplified and expressed in the tensor form as follows [27,28]: Mass conservation

Momentum equation

$$\frac{\partial(\rho * U_j)}{\rho u_j} = 0$$

Energy equation

$$\frac{\partial\left(U_J(T)\right)}{\partial X_J} = \frac{\partial}{\partial X_J}\left(\frac{\lambda}{\rho C_p}\frac{\partial T}{\partial X_j}\right)$$

The realizable k-e turbulence model [29,30] can provide the superior performance for flows involving rotation, boundary layer under strong adverse pressure gradients, separation, and recirculation, relative to the standard k-e model [31]. Ozden and Ilker [32] tried to use three turbulence models to simulate the flow and temperature characteristics of a STHX, of which results revealed that the realizable k-e model was the more suitable simulation approach. Consequently, it is determined as the turbulence model for all simulations in this work. Transport equations for the realizable k-e model are given as follows:

Turbulent kinetic energy k equation

$$\frac{\partial(\rho\kappa)}{\partial t} + \frac{\partial(\rho\kappa u_i)}{\partial xi} = \frac{\partial}{\partial xj}\left[\left(\mu\frac{\mu_t}{\sigma_k}\right)\frac{\partial k}{\partial x_j}\right] + G_K\text{-}\rho\varepsilon$$

where C1 and C2 are the model coefficients; rk and re are the turbulence Prandtl numbers for the k and e, respectively; Gk represents the producing item of the k by the mean velocity gradient, and it can be calculated as follows: 2.2.2. Boundary conditions The three-dimensional, double precision, pressure-based, and steady solver are adopted for the numerical computations by the commercial CFD software Fluent [31]. Governing equations are discretized with the finite volume formulation with the SIMPLE pressure-velocity coupling algorithm. The second order upwind scheme is chosen for the momentum, turbulent kinetic energy, turbulent dissipation rate, and energy, while the standard scheme is used for the pressure. Standard wall functions are adopted as the near-wall treatment, and the no-slip condition is applied to all solid walls. Water is selected as the working fluid, and its thermo-physical property parameters are temperature dependent as listed in Table 1.

Table 1 Thermo-physical property parameters of water. The inlet temperature of the water is set as a

Thermo-physical property parameters of water.

Item	Value (273 K < T < 373 K)
c_p, J·kg^{-1}·K^{-1}	10632.6–55.924 * T + 0.15968 * T^2-0.00014983 * T^3
μ, kg·m^{-1}·s^{-1}	0.11165–0.00095 T + 2.7424E–06 * T^2-2.6089E-09 * T^3
ρ, kg·m^{-3}	753.3 + 1.879 * T-0.00357 * T^2
λ, W·m^{-1}·K^{-1}	−2.58673 + 0.02399 * T−5.91953E−05 * T^2 + 4.92088E−08 * T^3

Table 1 : Thermo physical property of water.

constant of 293 K, and the temperature of the tube wall is maintained at 353 K, thus water is heated in the shell-side. The rest walls, including the shell, baffles, and tube sheets,

are adiabatic. The velocity inlet and outflow boundary conditions are adopted for the inlet and outlet, respectively. The inlet velocity ranges from 0.40 to 3.19 m/s in pace with the mass flow rate changing from 0.5 to 4 kg/s. The turbulence intensity I and turbulence length scale l are used as the turbulence specification method [31], and they are described as follows: where Rein and Din are the Reynolds number and inner diameter of the inlet, respectively.

2.4. Data reduction

The heat transfer rate Q via tube walls is calculated as

$Q = M\ C_p\ (T_{out} - T_{in})$

where Tout and Tin are the static temperatures of the inlet and outlet of the shell-side, respectively.

The heat transfer coefficient h can be expressed as

$$h = \frac{Q}{A\ \Delta T_m}$$

where A is the total heat transfer area, and DTm is the log mean temperature difference. They can be calculated by following expressions:

$A = N_t \pi\ p\ d\ L$

$$\Delta T_m = \frac{(T_W - T_{in}) - (T_W - T_{out})}{ln\,[(T_w - T_{in})/(T_w - T_{out})]}$$

where Nt is the number of tubes; Tw is the wall temperature of tubes.

The power consumption P caused by the flow resistance in the shell-side is defined as

$p = \Delta P\ V$

here, Dp is the pressure drop between the inlet and outlet; V is the volume flow rate of the working fluid.

III. CONCLUSIONS

A shell and tube heat exchanger with staggered baffles (STHXST) was proposed in this paper. The STHX-ST possessed the characteristics of the simple fabrication of the STHX-SG and the helical flow of the STHX-CH. Numerical analyses with respect to the heat transfer performance and pressure drop were conducted for the three STHXs. Effects of different parameters, including the baffle cut and the staggered angle, were studied for the STHX-ST. The conclusions can be summarized as follows: (1) With the regularly staggered arrangement of baffles, the helical flow is generated in the shell-side of the STHX-ST. (2) The comprehensive performance characterized by the relationship between the heat transfer rate and power consumption of the STHX-ST is superior to those of the STHXSG and STHX-CH. Namely, for the STHX-ST, the reduction of the heat transfer rate is cost-effective and meaningful considering the more significant decrease in the power consumption compared with the STHX-SG and STHX-CH. (3) The Pareto front for the heat transfer rate and pressure drop is obtained. The heat transfer rate under unit pressure drop Q/Dp reaches the summit for the STHX-ST at the d = 0. 49, b = 64_, and n = 7. The design variable for the d = 0. 45, b = 79_, and n = 11 is the optimal solution by the TOPSIS selection. (5) It is proved that the STHX-SG, a special STHX-ST at the b = 180_, is not always the best choice from the view of heat transfer enhancement. The STHX-ST can be considered to replace the STHX-SG at some applications from the perspective of the heat transfer enhancement. As a final point, it is safe to conclude that the STHX-ST proposed in this work provides a preferable and meaningful solution for more efficient energy utilization in industrial applications.

REFERANCE

[1] B.I. Master, K.S. Chunangad, A.J. Boxma, D. Kral, P. Stehlík, Most frequently used heat exchangers from pioneering research to worldwide applications, Heat Transf. Eng. 27 (2006) 4–11, https://doi.org/10.1080/01457630600671960

[2] K.J. Bell, Heat exchanger design for the process industries, J. Heat Transf. 126 (2004) 877–885, https://doi.org/10.1115/1.1833366.

[3] M. Prithiviraj, M.J. Andrews, Three dimensional numerical simulation of shelland-tube heat exchangers. Part I: foundation and fluid mechanics, Numer. Heat Transf. Part A Appl. 33 (1998) 799–816, https://doi.org/10.1080/ 10407789808913967.

[4] M. Prithiviraj, M.J. Andrews, Three-dimensional numerical simulation of shelland-tube heat exchangers. Part Ⅱ: heat transfer, Numer. Heat Transf. Part A Appl. 33 (1998) 817–828, https://doi.org/10.1080/10407789808913968

[5] M. Prithiviraj, M.J. Andrews, Comparison of a three-dimensional numerical model with existing methods for prediction of flow in shell-and-tube heat exchangers, Heat Transf. Eng. 20 (1999) 15–19.

[6] M.M. Aslam Bhutta, N. Hayat, M.H. Bashir, A.R. Khan, K.N. Ahmad, S. Khan, CFD applications in various heat exchangers design: A review, Appl. Therm. Eng. 32 (2012) 1–12, https://doi.org/10.1016/j.applthermaleng.2011.09.001.

[7] M.M. Elias, I.M. Shahrul, I.M. Mahbubul, R. Saidur, N.A. Rahim, Effect of different nanoparticle shapes on shell and tube heat exchanger using different baffle angles and operated with nanofluid, Int. J. Heat Mass Transf. 70 (2014) 289–297, https://doi.org/10.1016/j.ijheatmasstransfer.2013.11.018

[8] N. Ben Zheng, P. Liu, F. Shan, Z.C. Liu, W. Liu, Effects of rib arrangements on the flow pattern and heat transfer in an internally ribbed heat exchanger tube, Int. J. Therm. Sci. 101 (2016) 93–105, https://doi.org/10.1016/j. ijthermalsci.2015.10.035.

[9] Y.H. You, A.W. Fan, S.Y. Huang, W. Liu, Numerical modeling and experimental validation of heat transfer and flow resistance on the shell side of a shell-andtube heat exchanger with flower baffles, Int. J. Heat Mass Transf. 55 (2012) 7561–7569, https://doi.org/10.1016/j.ijheatmasstransfer.2012.07.058.

[10] J.J. Liu, Z.C. Liu, W. Liu, 3D numerical study on shell side heat transfer and flow characteristics of rod-baffle heat exchangers with spirally corrugated tubes, Int. J. Therm. Sci. 89 (2015) 34–42, https://doi.org/10.1016/j. ijthermalsci.2014.10.011.

[11] M. Saeedan, M. Bahiraei, Chemical engineering research and design effects of geometrical parameters on hydrothermal characteristics of shell-and-tube heat exchanger with helical baffles : Numerical investigation, modeling and optimization, Chem. Eng. Res. Des. 96 (2015) 43–53, https://doi.org/10.1016/j. cherd.2015.02.004.

[12] J. Lutcha, J. Nemcansky, Performance improvement of tubular heat exchangers by helical baffles, Chem. Eng. Res. Des. 68 (1990) 263–270.

[13] B.I. Master, K.S. Chunangad, V. Pushpanathan, Heat exchanger, US Patent No. 6827138, 2004.

[14] J.F. Zhang, B. Li, W.J. Huang, Y.G. Lei, Y.L. He, W.Q. Tao, Experimental performance comparison of shell-side heat transfer for shell-and-tube heat exchangers with middle-overlapped helical baffles and segmental baffles, Chem. Eng. Sci. 64 (2009) 1643–1653,https://doi.org/10.1016/j. ces.2008.12.018.

[15] J. Wen, H.Z. Yang, S.M. Wang, S.F. Xu, Y.L. Xue, H.F. Tuo, Numerical investigation on baffle configuration improvement of the heat exchanger with helical baffles, Energy Convers. Manage. 89 (2015)438–448,https://doi. org/10.1016/j.enconman.2014.09.059.

[16] D. Kral, P. Stehlik, H.J. Van Der Ploeg, B.I. Master, Helical Baffles in shell-andtube heat exchangers, Part I: experimental verification, Heat Transf. Eng. 17 (1996) 93–101, https://doi.org/10.1080/01457639608939868

[17] F. Nemati Taher, S. Zeyninejad Movassag, K. Razmi, R. Tasouji Azar, Baffle space impact on the performance of helical baffle shell and tube heat exchangers, Appl. Therm. Eng. 44 (2012) 143–149, https://doi.org/10.1016/j. applthermaleng.2012.03.042.

[18] Q.W. Wang, G.D. Chen, J. Xu, Y.P. Ji, Second-law thermodynamic comparison and maximal velocity ratio design of shell-and-tube heat exchangers with continuous helical baffles, J. Heat Transf. 132 (2010) 101801, https://doi.org/ 10.1115/1.4001755.

[19] Q.W. Wang, Q.Y. Chen, G.D. Chen, M. Zeng, Numerical investigation on combined multiple shell-pass shell-and-tube heat exchanger with continuous helical baffles, Int. J. Heat Mass Transf. 52 (2009) 1214–1222, https://doi.org/10.1016/j.ijheatmasstransfer.2008.09. 009.

[20] J.F. Yang, M. Zeng, Q.W. Wang, Numerical investigation on shell-side performances of combined parallel and serial two shell-pass shell-and-tube heat exchangers with continuous helical baffles, Appl. Energy 139 (2015) 163– 174, https://doi.org/10.1016/j.apenergy.2014.11.029.

[21] B. Peng, Q.W. Wang, C. Zhang, G.N. Xie, L.Q. Luo, Q.Y. Chen, M. Zeng, An experimental study of shell-and-tube heat exchangers with continuous helical baffles, J. Heat Transf. 129 (2007) 1425–1431, https://doi.org/10.1115/ 1.2754878.

[22] M. Mellal, R. Benzeguir, D. Sahel, H. Ameur, International journal of thermal sciences hydro-thermal shell-side performance evaluation of a shell and tube heat exchanger under different baffle arrangement and orientation, Int. J. Therm. Sci. 121 (2017) 138–149, https://doi.org/10.1016/j. ijthermalsci.2017.07.011.

[23] Y. Ge, Z.C. Liu, W. Liu, Multi-objective genetic optimization of the heat transfer for tube inserted with porous media, Int. J. Heat Mass Transf. 101 (2016) 981– 987, https://doi.org/10.1016/j.ijheatmasstransfer.2016.05. 118.

[24] M. Cavazzuti, M.A. Corticelli, Optimization of heat exchanger enhanced surfaces through multiobjective Genetic Algorithms, Numer. Heat Transf. Part A Appl. 54 (2008) 603–624, https://doi.org/10.1080/ 10407780802289335.

[25] A. Abdollahi, M. Shams, Optimization of heat transfer enhancement of nanofluid in a channel with winglet vortex generator, Appl. Therm. Eng. 91 (2015) 1116–1126, https://doi.org/10.1016/j.applthermaleng.2015.08.06 6.

[26] J. Yang, L. Ma, J. Bock, A.M. Jacobi, W. Liu, A comparison of four numerical modeling approaches for enhanced shell-and-tube heat exchangers with experimental validation, Appl. Therm. Eng. 65 (2014) 369–383, https://doi.org/ 10.1016/j.applthermaleng.2014.01.035.

[27] B.E. Launder, D.B. Spalding, The numerical computation of turbulent flows, Comput. Methods Appl. Mech. Eng. 3 (1974) 269–289, https://doi.org/10.1016/ 0045-7825(74)90029-2.

[28] H.K. Versteeg, W. Malalasekera, An introduction to computational fluid dynamics, Second Edi, 2007.

[29] T.H. Shih, J. Zhu, J.L. Lumley, A new Reynolds stress algebraic equation model, Comput. Methods Appl. Mech. Eng. 125 (1995) 287–302, https://doi.org/ 10.1016/0045-7825(95)00796-4.

[30] T.H. Shih, W.W. Liou, A. Shabbir, Z.G. Yang, J. Zhu, A new k-epsilon eddy viscosity model for high reynolds number turbulent flows, Comput. Fluids 24 (1995) 227–238, https://doi.org/10.1016/0045-7930(94)00032-T.

[31] FLUENT Inc, FLUENT User's Guide, Power, 2006.

[32] E. Ozden, I. Tari, Shell side CFD analysis of a small shell-and-tube heat exchanger, Energy Convers. Manage. 51 (2010) 1004–1014, https://doi.org/ 10.1016/j.enconman.2009.12.003.

[33] S.M. Salim, S.C. Cheah, Wall y+ strategy for dealing with wall-bounded turbulent flows, Int. MultiConference Eng. Comput. Sci. 2 (2009) 1–6,

doi: 10.1.1.149.722.

[34] K. Thulukkanam, Heat exchanger design handbook, Second Edi (2013), https:// doi.org/10.1201/b14877.

[35] K. Deb, A. Member, A. Pratap, S. Agarwal, T. Meyarivan, A fast and elitist multiobjective genetic algorithm: NSGA-Ⅱ, IEEE Trans. Evol. Comput. 6 (2002) 182–197.

[36] C.L. Hwang, K. Yoon, Multiple Attribute Decision Making Methods and Applications, first ed., Springer-Verlag Berlin Heidelberg, New York, 1981. doi:10.1007/978-3-642-48318-9.

